Manuscript Details

Manuscript number	MTENER_2016_49
Title	Ultrahigh energy density supercapacitors through a double hybrid strategy
Article type	Research Paper

Abstract

Herein, we are presenting all-solid-state symmetric supercapacitors (ASSSCs) with an innovative double hybrid strategy, where a hybrid electrode (reduced graphene oxide (rGO) anchored with phoshotungstic acid, rGO-H3PW12O40) is combined with redox-active species (hydroquinone-doped gel electrolyte) doped electrolytes. Initially, a hybrid electrode is fabricated by decorating H3PW12O40 nanodots onto the surface rGO (rGO-PW12). Later, an all-solid state symmetric cell was assembled with rGO-PW12 electrodes and PVA-H2SO4 polymer gel-electrolyte. Interestingly, rGO-PW12 symmetric cell revealed a substantial enhancement in the cell performance as compared to parent rGO systems. It featured a widened potential range of 1.6 V which provides an energy density of 1.05 mWh/cm3. In order to further improve the performance of rGO-PW12 cell, we have introduced redox-active (hydroquinone) species in to the polymer gel-electrolyte. The performance of rGO-PW12 cell was surprisingly improved with an ultra-high energy density of 2.38 mWh/cm3 (more than two-fold).

Keywords	Reduced graphene oxide-phosphotungstate hybrid; Hydroquinoe-doped gel electrolyte; Symmetric supercapacitors

Corresponding Author	Deepak Dubal
Corresponding Author's Institution	Catalan Institute of Nanoscience and Nanotechnology, CIN2, ICN2 (CSIC-ICN)
Order of Authors	Deepak Dubal, Bhawna Nagar, Pedro Gomez-Romero
Suggested reviewers	Keryn Lian, Rudolf Holze, Y.P. Wu

Submission Files Included in this PDF

File Name [File Type]

Cover letter.docx [Cover Letter]

Graphical Abstract.docx [Graphical Abstract]

Manuscript_Gr-Tung_Final.doc [Manuscript File]

Figures PW12_NC.doc [Figure]

Supporting information.doc [e-Component]

Highlights.docx [Highlights]

To view all the submission files, including those not included in the PDF, click on the manuscript title on your EVISE Homepage, then click 'Download zip file'.

Date: 23 Nov. 16

To,

The Editor,

Materials Today Energy

Dear Editor,

This letter implies online submission of our recent invention entitled **"Ultrahigh energy density supercapacitors through a double hybrid strategy"** by *Deepak P. Dubal,[a]* Bhawna Nagar,[a] Pedro Gomez-Romero [a]*** for publication in ***Materials Today Energy***

In the race of new advanced electrode materials for high energy density supercapacitors, the promising materials such as polyoxometalates are slightly ignored. POMs are molecular oxides cluster molecule and holds promise to achieve high capacity for energy storage applications due to their fast and reversible multi-electron redox reactions.

Here, we are presenting fabrication of all-solid state symmetric supercapacitors (ASSSc) based on double hybrid approach combining a hybrid electrode (reduced graphene oxide-phoshotungstate, rGO-PW_{12}) and a hybrid electrolyte (hydroquinone doped gel-electrolyte). To begin with, a high-performance hybrid electrode based on $H_3PW_{12}O_{40}$ nanodots anchored onto rGO was prepared (rGO-PW_{12}). Later, an all-solid state symmetric cell based on these rGO-PW_{12} electrodes, and making use of a polymer gel-electrolyte was assembled. This symmetric cell showed a significant improvement in cell performance. Indeed, it allowed for an extended potential window by 0.3 V which led to an energy density of 1.05 mWh/cm^3.

In addition, we have extended our work dedicating earnest efforts to investigate the effect of addition of redox-active species (hydroquinone in this particular case) in the gel electrolyte to further improve the performance of rGO-PW_{12} solid-state symmetric capacitors.

The Quinone/Hydroquinone (Q/HQ) redox couple of p-benzoquinone is highly reversible and undergoes a 2-electron redox process. Strikingly, a further 2-fold increase in the device performance was realized with the hybrid electrodes-hybrid electrolyte combination cell as compared to the conventional electrolyte cell.

I really hope you will agree that this excellent report could be a seminal article for many interesting reports to come. I look forward to your news

Best Regards

Dr. Deepak P. Dubal, Ph. D.

Marie-Curie Fellow (BP-DGR), (AvH, Germany)

Catalan Institute of Nanoscience and Nanotechnology, CIN2, ICN2 (CSIC-ICN)

Campus UAB, E-08193 Bellaterra (Barcelona), Spain

TOC

Schematic illustration of double hybridization approach with corresponding STEM and SEM images of hybrid electrodes

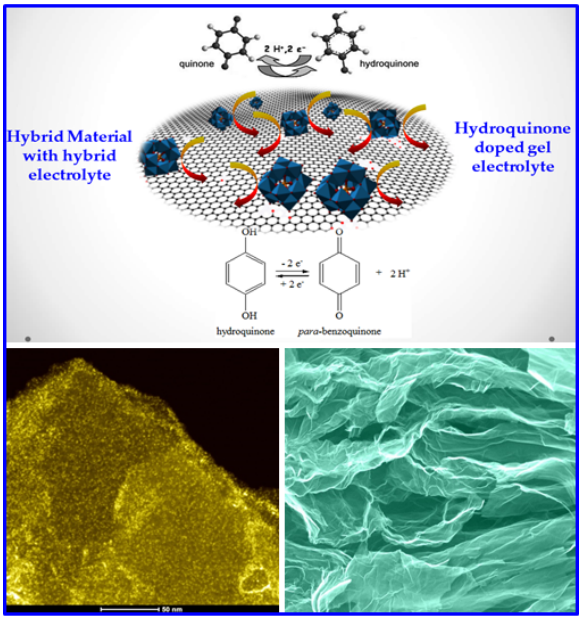

Ultrahigh energy density supercapacitors through a double hybrid strategy

Deepak P. Dubal, Bhawna Nagar, Pedro Gomez-Romero***

[a]Catalan Institute of Nanoscience and Nanotechnology (ICN2), CSIC and The Barcelona Institute of Science and Technology, Campus UAB, Bellaterra, 08193 Barcelona, Spain

CORRESPONDING AUTHOR FOOTNOTE

Dr. Deepak Dubal, and Prof. Pedro Gomez-Romero

Tel.: +349373609/+345929950 Fax: +345929951

E-mail: dubaldeepak2@gmail.com (D. Dubal),

pedro.gomez@cin2.es (P. Gomez-Romero)

Abstract

Herein, we are presenting all-solid-state symmetric supercapacitors (ASSSCs) with an innovative double hybrid strategy, where a hybrid electrode (reduced graphene oxide (rGO) anchored with phoshotungstic acid, rGO-$H_3PW_{12}O_{40}$) is combined with redox-active species (hydroquinone-doped gel electrolyte) doped electrolytes. Initially, a hybrid electrode is fabricated by decorating $H_3PW_{12}O_{40}$ nanodots onto the surface rGO (rGO-PW_{12}). Later, an all-solid state symmetric cell was assembled with rGO-PW_{12} electrodes and PVA-H_2SO_4 polymer gel-electrolyte. Interestingly, rGO-PW_{12} symmetric cell revealed a substantial enhancement in the cell performance as compared to parent rGO systems. It featured a widened potential range of 1.6 V which provides an energy density of 1.05 mWh/cm^3. In order to further improve the performance of rGO-PW_{12} cell, we have introduced redox-active (hydroquinone) species in to the polymer gel-electrolyte. The performance of rGO-PW_{12} cell was surprisingly improved with an ultra-high energy density of 2.38 mWh/cm^3 (more than two-fold).

Keywords: Reduced graphene oxide-phosphotungstate hybrid, Hydroquinoe-doped gel electrolyte, Symmetric supercapacitors, Ultrahigh energy density

1. Introduction

Energy storage technologies are quickly maturing in order to effectively grow as key players in the forthcoming sustainable energy model. Electrical energy storage in particular will have to widen its target performance evolving from consumer electronics to a much broader set of applications, including grid, load-leveling, electric vehicles and other high-power applications. New materials, new devices and new systems will significantly contribute to satisfy this widened growth by making possible faster, more durable and cheaper high energy-density storage [1].

Combining high energy and power in a single device is a holy grail in energy storage but not an easy one to get through circuitry at a low price. Thus, materials and very especially electrode materials have been explored to increase their intrinsic energy and power densities by means of various approaches from nanostructured design to hybridization. Nanostructure is a good way to increase and optimize electrode-electrolyte interfaces, whereas the development of hybrid materials allows for harnessing complementary properties of the components and even emerging synergic performances. Of course these two approaches are not incompatible and can be used altogether reinforcing each other [1, 2]. Indeed, there is a strong and growing research area dealing with hybrid nanocomposite materials for energy storage applications [1].

Polyoxometalates (POMs) are clusters of anionic molecular metal oxide which includes early transition metals (e.g. V, Mo, W) in their highest oxidation states. They have been well known in the realm of inorganic chemistry for a long time [3] but only recently have been recognized as useful nanosized blocks for the design of functional materials with outstanding applications in catalysis, energy conversion and molecular electronics [4-6]. Within the field of energy storage, they have found a particularly well-suited niche application in supercapacitors, initially integrated in conducting polymers

[7-9] and more recently forming hybrid electrodes with carbon materials [10-14]. POMs can exhibits high energy density for supercapacitors due to the rapid and reversible multi-electron redox reactions. However the electrical connection of POMs trough conducting substrates is crucial to maximize their electron-transfer activity while preventing the dissolution of these clusters in the electrolytes. Therefore researchers are currently exploring the anchoring of POMs on nanocarbons (carbon nanotubes CNTs, graphene etc.) to immobilize and integrate POMs in electrically conducting substrates. Keggin's structure is the smallest and simplest version of POMs which electrochemically active and stable in aqueous acidic-media [15].

We first prepared a new hybrid electrode material based on Phosphotungstic acid ($H_3PW_{12}O_{40}$, in short, PW_{12}) and reduced Graphene Oxide (rGO). As it will be shown, these materials present a synergic combination with a dual charge storage mechanism: electrical double layer (EDL, nanocarbons) and redox (faradaic, PW_{12}). Related hybrid electrodes formed by Activated Carbons (AC) and polyoxometalates have shown how the anchoring of the inorganic clusters onto the carbon microporous surface effectively leads to increased (capacitive + faradaic) electrochemical activity of the electrodes and to enhanced performance of symmetrical supercapacitor devices [11, 12].

In addition to the preparation of these hybrid electrode materials we went one step further and tested the use of a hybrid electrolyte, that is, a gel electrolyte containing redox-active hydroquinone in addition to protons (1M aqueous H_2SO_4) in order to achieve more advancement in rGO-PW_{12} based device performance. The use of electroactive redox species in EDLC supercapacitor electrolytes has been studied earlier, for instance using the I^-/I_3^- redox couple [16]. In the present paper though we have tried and report a specific combination of electrode and electrolyte, both incorporating different but compatible redox-active species.

2. Methods

2.1 Fabrication of rGO-PW_{12} hybrid materials based

Starting with the preparation of graphene oxide (GO) using a modified Hummers method: 2.5 g sodium nitrate ($NaNO_3$) was mixed with 125 ml of sulfuric acid (H_2SO_4) with continuous stirring. To which, 2.5 g graphite powder was added and stirred for 30 min in an ice bath. Later, 12.5 g of potassium permanganate ($KMnO_4$) was added to the above solution, and then the solution was maintained at 50 °C for 2 h with constant stirring. In the next step, 500 ml deionized water and 15 ml of hydrogen peroxide (H_2O_2) (35%) were added slowly to the resulting solution, and the solution was washed with dilute HCl. Finally, the GO product was washed again with 250 ml concentrated HCl (37%). The reduced graphene oxide (rGO) was prepared by high temperature treatment of the GO at 800 °C under nitrogen for 1 hr.

Later, a hybrid material based on rGO and phosphotungstate (rGO-PW_{12}) was prepared as follows: 0.25 g of rGO was dispersed in 100 ml of deionized water with a probe sonicator for 1 h. Later, 10 mM phosphotungstic acid ($H_3PW_{12}O_{40}\cdot 3H_2O$, ($PW_{12}$)) was mixed to the above pre-sonicated 100 ml rGO dispersion. This suspension was sonicated for 5 h in bath sonicator and maintained at room temperature for 24 h. Finally, the product was filtered off and dried in vacuum oven at 80 °C overnight.

2.2 Electrochemical measurements

The pastes were prepared with the formulation of 85 % of active material (rGO or rGO-PW_{12}: 10 % PVDF as binder: 5 % Super P acetylene black. A small amount of N-Methyl-2-pyrrolidone as solvent was added and the mixture was stirred for 24 h in order to prepare homogeneous paste. Finally, the paste was coated on carbon cloth with doctor-blade method which was further used as an electrode. All-solid state symmetric cells were fabricated using Swagelok® cells with two rGO-PW_{12} electrodes of the same

mass and H_2SO_4/Polyvinyl alcohol (PVA) gel electrolyte assembled under pressure. The electrochemical properties all the devices were tested out using a Biologic VMP3 potentiostat.

3. Results and Discussion

3.1 Synthesis and characterizations

We have used reduced graphene oxide (rGO) with a three-dimensional (3D) interconnected open porous nanosheets prepared by a modified Hummers' method as our base capacitive material. Subsequently, phosphotungstic acid ($H_3PW_{12}O40$) was uniformly and effectively decorated on the rGO nanosheets as it is shown in Figure 1, which shows ultrathin graphene nanosheets decorated with tiny yet numerous PW_{12} clusters (1 nm in size).

Further, the electrochemical performance of rGO-PW_{12} was studied by fabricating symmetrical supercapacitors with H_2SO_4/Polyvinyl alcohol (PVA) gel electrolyte.

XRD patterns of rGO and rGO-PW_{12} hybrid materials shown in Figure 2 (a) suggests two well-resolved peaks at 25.6º and 42.5º for both materials which can assigned to (002) and (001) planes, respectively [17]. Interestingly, no additional peak corresponding to PW_{12} is observed, suggesting uniform distribution of the molecular PW_{12} clusters on the surface of rGO. Moreover, the broad and low intensity peaks for the rGO-PW_{12} hybrid further confirms poor long-range order as compared to the rGO due to the anchoring of the inorganic clusters.

Two major and common peaks at 284.5 eV and 533.5 eV are observed in the overview of XPS spectra for rGO and rGO-PW_{12} which corresponds to C1s and O1s, respectively (Supporting information S1a). On the other hand, rGO-PW_{12} sample

exhibits an additional peak at 35.71 eV (4f) which is assigned to tungsten. It is further interesting to note that, the peak intensity of core-level C1s spectra is considerably decreased with a minor shift towards low binding energy for rGO-PW_{12} (see Figure 2b). Furthermore, core-level W4f spectrum shows two peaks at 37.54 eV ($W4f_{5/2}$) and 35.4 eV ($W4f_{7/2}$) with spin-orbit splitting of 2.14 eV (with a peak ratio 4:3). Thus, it is revealed that W atoms are in W(VI) oxidation state, confirming the presence of fully oxidized PW^{VI}_{12} in rGO-PW_{12} hybrid (Figure 2c) [18, 19].

The morphological analyses were performed in order to confirm and further characterize the anchoring of PW_{12} onto the surface of open-porous interconnected network of rGO nanosheets. SEM images of rGO and rGO-PW_{12} hybrid materials are presented in Figure 2 (d, e), respectively. It is evidenced that, rGO possesses interconnected ultrathin nanosheets which forms three dimensional open porous architectures. This unique nanoarchitecture can provide highly conducting framework which is extremely favorable to enhance the electron transport. It is further interesting to note that, the open-porous structure of rGO is still maintained even after heavy decoration of PW_{12} clusters (see Figure 2e). The detailed analysis of PW_{12} anchoring on to the rGO surface was further investigated with STEM and displayed in Figure 2 (f, g). The surface of rGO looks more smooth and dustless as seen from Figure 2 (f) while on the complete contrary, huge number of white tiny dots of around nanometers size are clearly seen for rGO-PW_{12} hybrid (Figure. 2 g). Notably, the PW_{12} nanodots are uniformly anchored on to the surface of rGO nanosheets. Furthermore, black tiny nanoparticles of PW_{12} are clearly observed (few of them are marked with white circles) in HR-TEM image for rGO-PW_{12} hybrid (Figure 2 (h)). EDS mapping of rGO-PW_{12} hybrid (see Figure 2 (i)) further confirms the presence of 1 nm sized PW_{12} nanodots uniformly decorated on to the surface of rGO nanosheets (see supporting Figure. S1b).

We should keep in mind that all the twelve WO_6 species are on the surface in 1 nm sized PW_{12} clusters, underscoring the ultimate dispersion of the electroactive clusters in rGO-PW_{12} hybrids. Also, it is well known that the charges stored in the pseudo-capacitive materials rely on the surface redox reactions which means the energy is stored through the charge transfer near the electrode surface. In this context, the rGO-PW_{12} hybrid presented here is an ideal material which is a rational combination of open porous interconnected rGO nanosheets with redox active PW_{12} molecular clusters, thereby providing an exclusive foundation from a structural point of view.

The hybrid materials with excellent surface area and open-porosity are crucial parameters in order to achieve high performance electrode materials for supercapacitors. The BET surface area for rGO and rGO-PW_{12} samples were found to be 242 m^2/g and 237 m^2/g, respectively (supporting information S2a). The negligibly small decrease in the BET surface area for rGO-PW_{12} samples might be ascribed to the anchoring of PW_{12} clusters, which considerable improves the final mass of the hybrid material. However, rGO-PW_{12} hybrid material still exhibits excellent BET surface area which is significantly higher than the reported carbon based hybrid materials [3, 20, 21]. It is further seen that, both rGO and rGO-PW_{12} samples exhibit mesoporous nature (supporting information S2b), showing a pores in the range of 2-8 nm. Moreover, it is worth noting that there is substantial increase in the pore volume of rGO from 0.10 cm^3/g to 0.16 cm^3/g after anchoring the PW_{12} molecular cluster which can offer easy path for ion insertion/de-insertion into the hybrid electrode.

Further, the rGO and rGO-PW_{12} hybrid electrodes were tested by assembling all-solid state symmetric cells with H_2SO_4/PVA gel electrolyte. Figure 3 (a, b) summarizes the electrochemical properties of rGO and rGO-PW_{12} symmetric cells. The CV curves for rGO and rGO-PW_{12} cells at a fixed scan rate of 20 mV/s are presented in Figure 3

(a). The anchoring of PW_{12} on the surface of rGO nanosheets dramatically improves the current density with an additional working voltage of 0.3 V than that for rGO based cell. Likewise, the rGO-PW_{12} cell exhibits noticeably longer discharging time as seen in Figure 3 (b), indicating a significantly greater specific capacitance. The larger working voltage (up to 1.6 V) of rGO-PW_{12} will lead to improved energy density of the cell. These excellent electrochemical properties can be assigned to the combined contribution from rGO (EDLC) and PW_{12} (faradic) in hybrid material. The CV curves for rGO-PW_{12} cell at various scan rate are displayed in Figure 3 (c). The shapes of CV curves are quasi-rectangular with strong redox peaks due to the faradic PW_{12} clusters overlapped with capacitive contribution from rGO which are extremely unlike than that for rGO based cell (supporting information S3). These CV shapes correspond to the combined charge storing mechanisms, faradaic (PW_{12}) and capacitive (EDLC). Moreover, the rGO-PW_{12} cell retains their shapes of CV curves at high scan rate of 100 mV/s, suggesting excellent rate capability of rGO-PW_{12} cells for rapid charge and discharge. Galvanostatic charge/discharge measurements were carried out at different current densities for rGO-PW_{12} based cell and shown in Figure 3 (d). The non-triangular shapes of GCD curves for rGO-PW_{12} cell further suggests the inclusion of both charge storing mechanisms i.e. capacitive from rGO and faradic from PW_{12}. Moreover, in case of both cells, there is very small initial voltage drop, indicating low internal resistance of both electrodes materials. In addition, the charging parts are almost symmetrical to their counter discharging parts, suggesting rapid and excellent electrochemical reversibility. For detailed calculations of electrochemical properties see supporting information S4. The plots of volumetric capacitances with respect to current density for both rGO and rGO-PW_{12} cells are shown in Figure 3 (e). The volumetric capacitance for rGO-PW_{12} cell was calculated to be 2.95 F/cm^3 (260 mF/cm^2) and 1.1 F/cm^3 (96 mF/cm^2) at 1.27

and 25.47 mA/cm^2 applied current densities, respectively. These values are significantly higher than that for rGO cell (0.7 F/cm^3 (60 mF/cm^2) and 0.33 F/cm^3 (28 mF/cm^2) at current density of 1.27 and 10.2 mA/cm^2, respectively). The whole credit for this great increase in specific capacitance goes to the redox contribution of PW_{12} clusters in the hybrid material. Furthermore, the cells retained around 32 % (rGO) and 35 % (rGO-PW_{12}) of initial capacitance after increase in scan rate from 5 to 100 mV/s, suggesting good rate capability of both the systems. There is obvious decrease in the specific capacitance values with scan rate which might be assigned to the slower electrochemical kinetics at higher scan rates. The capacitance values achieved in present investigation are extensively higher than the literature values for symmetric as well as asymmetric cells [7, 8, 21-23] and solid state gels based on metal oxides [24-29] (supporting information S5). The energy and power densities were calculated for both rGO and rGO-PW_{12} cells and shown in Figure 3 (f). As seen in the Ragone plots, the rGO-PW_{12} cell provides maximum energy density of 1.05 mWh/cm^3 at power of 11.5 mW/cm^3 which is significantly higher than that for rGO based cells (0.2 mWh/cm^3 at power of 9 mW/cm^3). Impressively, at a high power density of 231.6 mW/cm^3, the rGO-PW_{12} cell still delivers energy density of 0.4 mWh/cm^3 which is higher than rGO based cell. Thus, the results obtained here suggests that an innovative rGO-PW_{12} hybrid material is robust candidates to design high power and high energy supercapacitors. In addition, the symmetric cell design provides better results as compared to the complex asymmetric designs.

3.2 Effect of hydroquinone doping in gel-electrolyte

Recently, some interesting investigation showed the advancement in supercapacitive performance of electrodes using redox/active electrolytes [30, 31] in particular conducting polymers [30]. In our recent investigation, we proved that, the

inclusion of redox active species (hydroquinone) in gel-electrolyte significantly improves the performance of rGO-PMo_{12} symmetric device [32]. Herein, we are exploring the similar concept to further advance the supercapacitive performance of rGO-PW_{12} cell with redox-active species (hydroquinone) added PVA/H_2SO_4 gel-electrolyte. The p-benzoquinone exhibits a redox couple of Quinone/Hydroquinone (Q/HQ) which is highly reversible, 2-electron redox process. The hybrid gel-electrolytes were prepared with three different concentrations of hydroquinone. The CV curves for rGO-PW_{12} cell with 0.2 M HQ added polymer gel-electrolyte are shown in Figure 4 (a). Strikingly, the shapes of CV curves are completely different than that observed with the conventional gel-electrolyte and shows very strong redox peaks, suggesting extra-ordinary improvement in the device performance. Obviously, this excellent advancement can be attributed to the Q/HQ redox reactions of p-benzoquinone which not only added redox species but also provides additional protons, thereby offers extra reaction sites for rapid and reversible redox reactions [32].

The maximum area under the CV curves i.e. the maximum current density is obtained for rGO-PW_{12} cell with 0.2 M HQ doped gel-electrolyte which starts to decrease for higher concentration of HQ (supporting information S6). Likewise, the charge/discharge times for rGO-PW_{12} cell gradually increases till 0.2 M HQ which decreases for further increase in HQ concentration as shown in Figure 4 (b-d). The volumetric capacitance of rGO-PW_{12} cells at various current densities for all HQ concentrations were calculated and plotted in Figure 4 (e). The volumetric capacitances calculated for rGO-PW_{12} with 0.2 M HQ gel-electrolyte is 6.72 F/cm^3 (592 mF/cm^2) and 1.33 F/cm^3 (117 mF/cm^2) at current densities of 1.27 mA/cm^2 and 25.47 mA/cm^2, respectively, significantly higher than that with conventional gel-electrolyte. There is

apparent decrease in the capacitance with current density which might be assigned to the slower kinetics at higher current densities (supporting information S7 and S8).

Thus, a double hybridization approach where rGO-PW_{12} hybrid electrode with redox-active species added hybrid gel electrolyte effectively enhances the performance of the device. The energy and power densities are shown in the Ragone plots (see Figure 4 (f)). The energy densities for rGO-PW_{12} cell are found to be 1.22 mWh/cm^3 (11.81 Wh/kg), 2.39 mWh/cm^3 (23.11 Wh/kg) and 1.61 mWh/cm^3 (15.61 Wh/kg) at a fixed power density of 11.58 mW/cm^3 (112 W/kg) for 0.1 M, 0.2 M and 0.3 M HQ concentrations, respectively. Surprisingly, at high power density of 232 mW/cm^3 (2.23 kW/kg), rGO-PW_{12} cell with hybrid gel-electrolyte delivers decent energy density values in the range of 0.4-0.8 mWh/cm^3, confirming the great potential for high energy and high power applications. Compared to the literature values reported for gel-electrolytes, present investigation offers excellent performances [24-26, 28, 29, 32-35]. Thus, this innovative investigation open new opportunities for the further development of high performance supercapacitors.

The practical application of rGO-PW_{12} cell with redox-active electrolyte is demonstrated by illuminating LEDs. The word "NEO" (NEO is short form of our group's name, Novel Energy Oriented-Materials) of 31 LEDs is lit by single rGO-PW_{12} cell with 0.2 M HQ added gel-electrolyte for almost 120 secs after a short full-charging time of ~30 s, suggesting excellent energy output on fast charging (see Figure 5). The reasons for this excellent electrochemical performances are listed as follows: 1) hybrid electrode, which is a combination of two best materials of two different charge storing mechanisms i.e. EDLC (rGO) and faradaic (PW_{12}), 2) open-porous interconnected rGO nanosheets offers conducting channels for fast ionic transport, 3) excellent redox contribution from homogeneously anchored quantum sized PW_{12} molecular clusters 3)

Large operational working voltage window (1.6 V) provided by unique cell design rGO-PW_{12}/PVA-H_2SO_4/rGO-PW_{12}, resulting in enhanced energy density, 4) Hybrid electrolyte: incorporation of H/HQ redox active species in polymer gel-electrolyte certainly provides extra protons as well as additional faradaic active sites for energy storage. Certainly, HQ incorporation offers a molecular species which can be reversibly oxidized at the positive electrode during charge, counterbalancing the simultaneous faradaic reduction of PW_{12} at the negative electrode in a battery-like arrangement adding further energy density to the device.

4. Conclusions

We have effectively explored a concept of double hybridization in all solid state supercapacitors including: i) design and synthesis of hybrid electrode by anchoring redox-active PW_{12} molecular clusters onto the surface of rGO nanosheets, and ii) applying a hybrid gel-electrolyte formulation incorporating redox-active hydroquinone species to a conventional H_2SO_4 electrolyte. With the conventional gel-electrolyte, the symmetric cell based on rGO-PW_{12} hybrid shows considerable enhancement in the device performance, providing wider voltage window up to 1.6 V, which delivers an energy density of 1.05 mWh/cm^3. Furthermore, an incorporation of redox-active HQ into a gel electrolyte extra-ordinarily improves the performance of rGO-PW_{12} based device. Remarkably, a 2-fold increase in the device performance (energy density of 2.38 mWh/cm^3) is achieved after introduction of redox-active species. Thus, overall results ensure that the double hybrid approach (rGO-PW_{12} hybrid electrode) and hybrid electrolyte (redox-active) is promising for the development of high performance supercapacitors.

Associated Content

Supporting Information

The Supporting Information is available free of charge on the ACS Publications website. Additional details of FESEM analysis of full XPS spectra and TEM image of pristine, BET analysis of rGO and rGO-PW_{12} samples. In addition, CV and Cd curves of rGO at different scan rate and current densities are provided. Methods used for the calculation of electrochemical parameters. **Table S5** Comparison on supercapacitive values of POM as well as metal oxide based electrodes. Plots of electrochemical parameters for rGO and rGO-PW_{12} samples at different hydroquinone doped gel-electrolytes.

Acknowledgments

Partial funding from Miisterio de Economía y Competitividad through Fondo Europeo de Desarrollo Regional (FEDER) (Grant MAT2015-68394-R, MINECO/FEDER) and from AGAUR (project NESTOR) are acknowledged. ICN2 acknowledges support of the Spanish MINECO through the Severo Ochoa Centers of Excellence Program under Grant SEV-2013-0295. Finally, the award to DPD of a Marie-Curie Fellowship through Beatriu de Pinos Program (BP-DGR-2013) from the Catalan system of science and technology, Spain, is gratefully acknowledged

References

[1] Dubal, D. P.; Ayyad, O.; Ruiz, V.; Gómez-Romero, P. Hybrid Energy Storage: The Merging of Battery and Supercapacitor Chemistries. *Chem. Soc. Rev.* **2015**, *44*, 1777–1790

[2] Simon, P.; Gogotsi, Y.; Dunn, B.; Where Do Batteries End and Supercapacitors Begin? *Science*, **2014**, 343,1210-1211

[3] Baker, L. C. W.; Glick, D. C.; Present General Status of Understanding of Heteropoly Electrolytes and a Tracing of Some Major Highlights in the History of Their Elucidation, *Chem. Rev.* **1998**, 98, 3-50.

[4] Gomez-Romero, P.; Polyoxometalates as Photoelectrochemical Models for Quantum-Sized Semiconducting Oxides, *Sol. State Ionics* **1997**, 101, 243-248

[5] Long, D.-L.; Tsunashima, R.; Cronin, L.; Polyoxometalates: building blocks for functional nanoscale systems, *Angew. Chem. Int. Ed.* **2010**, 49, 1736-1758

[6] Ji, Y.; Huang, L.; Hu, J.; Streb, C.; Song, Y. F.; Polyoxometalate-Functionalized Nanocarbon Materials for Energy Conversion, Energy Storage and Sensor Systems, *Energy Environ. Sci.*, **2015**, 8, 776-789

[7] Gomez-Romero, P.; Chojak, M.; Cuentas-Gallegos, K.; Asensio, J. A.; Kulesza, P. J.; Casan-Pastor, N.; Lira-Cantu, M. Hybrid Organic-Inorganic Nanocomposite Materials for Application in Solid State Electrochemical Supercapacitors, *Electrochem. Commun.* **2003**, 5, 149-153.

[8] Cuentas-Gallegos, A. K.; Lira-Cantu, M.; Casan-Pastor, N.; Gomez-Romero P.; Nanocomposite Hybrid Molecular Materials for Application in Solid-State Electrochemical Supercapacitors, *Adv. Funct. Mater.* **2005**, 15, 1125-1133.

[9] Vaillant, J.; Lira-Cantu, M.; Cuentas-Gallegos, K.; Casan-Pastor, N.; Gomez-Romero, P.; Chemical Synthesis of Hybrid Materials based on PAni and

PEDOT with Polyoxometalates for Electrochemical Supercapacitors, *Prog. Sol. State Chem.* **2006**, 34, 147-159.

[10] Cuentas-Gallegos, A.; Martinez-Rosales, R.; Baibarac, M.; Gomez-Romero, P.; Rincon, M. E.; Electrochemical Supercapacitors Based on Novel Hybrid Materials Made of Carbon Nanotubes and Polyoxometalates, *Electrochem. Commun.* **2007**, 9, 2088-2092.

[11] Ruiz, V.; Suarez-Guevara, J.; Gomez-Romero, P.; Hybrid Electrodes Based on Polyoxometalates-Carbon Materials for Electrochemical Supercapacitors. *Electrochem. Commun.*, **2012**, 24, 35-38.

[12] Suarez-Guevara, J.; Ruiz, V.; Gomez-Romero, P.; Hybrid Energy Storage: High Voltage Aqueous Supercapacitors Based on Activated Carbon-Phosphotungstate Hybrid Materials, *J. Mater. Chem. A*, **2014**, 2, 1014-1021

[13] Genovese, M.; Lian, K.; Pseudocapacitive Behavior of Keggin Type Polyoxometalate Mixtures, *Electrochem. Commun.*, **2014**, 43, 60-62.

[14] Genovese, M.; Lian, K.; Polyoxometalate Modified Inorganic-Organic Nanocomposite Materials for Energy Storage Applications: A Review, *Curr. Opin. Solid State Mater. Sci.* **2015**, 19, 126-137

[15] Casan-Pastor, N.; Gomez-Romero, P.; Polyoxometalates: From Inorganic Chemistry to Materials Science, *Front. Biosci.* **2004**, 9, 1759-1770.

[16] Lota, G.; Fic, K.; Frackowiak, E.; Alkali Metal Iodide/Carbon Interface as a Source of Pseudocapacitance, *Electrochem. Commun.* **2011**, 13, 38-41

[17] Kim, H.; Park, K. Y.; Hong, J.; Kang, K.; All-Graphene-Battery: Bridging the Gap between Supercapacitors and Lithium Ion Batteries. *Sci. Rep.*, **2014**, 4 : 5278

[18] Barreca, D.; Carta, G.; Gasparotto, A.; Rossetto, G.; Tondello, E.; Zanella, P,; A

Study of Nanophase Tungsten Oxides Thin Films by XPS. *Surf. Sci. Spectra*, **2001**, 8, 258

[19] Weinhardt, L.; Blum, M.; Bär, M.; Heske, C.; Cole, B.; Marsen, B.; Miller, E. L.; Electronic Surface Level Positions of WO_3 Thin films for Photoelectrochemical Hydrogen Production. *J. Phys. Chem. C,* **2008**, 112, 3078-3082.

[20] Wei, W.; Cui, X.; Chen, W.; Ivey, D. G.; Manganese Oxide-Based Materials as Electrochemical Supercapacitor Electrodes. *Chem. Soc. Rev.*, **2011**, 40, 1697-1721

[21] Chen, H. Y.; Al-Oweini, R.; Friedl, J.; Lee, C. Y.; Li, L.; Kortz, U.; Stimming, U.; Srinivasan, M.; A Novel SWCNT-Polyoxometalate Nanohybrid Material as an Electrode for Electrochemical Supercapacitors. *Nanoscale*, **2015**, 7, 7934-7941.

[22] Skunik, M.; Chojak, M.; Rutkowska, I. A.; Kulesza, P. J.; Improved Capacitance Characteristics During Electrochemical Charging of Carbon Nanotubes Modified with Polyoxometallate Monolayers. *Electrochim. Acta*, **2008**, 53, 3862-3869.

[23] Suppes, G. M.; Cameron, C. G.; Freund, M. S.; A Polypyrrole/Phosphomolybdic Acid//Poly(3,4-ethylenedioxythiophene)/Phosphotungstic Acid Asymmetric Supercapacitor. *J. Electrochem. Soc.,* **2010**, 157**,** A1030-A1034

[24] Lu, X.; Zeng, Y.; Yu, M.; Zhai, T.; Liang, C.; Xie, S.; Balogun, M; Tong, Y.; Oxygen-Deficient Hematite Nanorods as High-Performance and Novel Negative Electrodes for Flexible Asymmetric Supercapacitors. *Adv. Mater.* **2014**, *26*, 3148-3155.

[25] Yang, P.; Xiao, X.; Li, Y.; Ding, Y.; Qiang, P.; Tan, X.; Mai, W.; Lin, Z.; Wu, W.; Li, T.; Jin, H.; Liu, P.; Zhou, J.; Wong, C. P.; Wang, Z. L.; Hydrogenated ZnO Core-Shell Nanocables for Flexible Supercapacitors and Self-Powered Systems. *ACS Nano* **2013**, 7, 2617-2626

[26] Lu, X. H.; Wang, G. M.; Zhai, T.; Yu, M. H.; Xie, S. L.; Ling, Y. C.; Liang, C. L.; Tong, Y. X.; Li, Y.; Stabilized TiN Nanowire Arrays for High-Performance and Flexible Supercapacitors. *Nano Lett.* **2012**, 12, 5376-5381.

[27] El-Kady, M. F.; Strong, V.; Dubin, S.; Kaner, R. B.; Laser Scribing of High-Performance and Flexible Graphene-Based Electrochemical Capacitors. *Science* **2012**, 335, 1326-1330.

[28] Zilong, W.; Zhu, Z.; Qiu, J.; Yang, S.; High Performance Flexible Solid-State Asymmetric Supercapacitors from MnO_2/ZnO Core–Shell Nanorods//Specially Reduced Graphene Oxide. *J. Mater. Chem. C,* **2014**, 2, 1331-1336.

[29] Lu, X.; Yu, M.; Wang, G.; Zhai, T.; Xie, S.; Ling, Y.; Tong, Y.; Li, Y.; H-TiO_2@MnO_2//H-TiO_2@C Core-Shell Nanowires for High Performance and Flexible Asymmetric Supercapacitors. *Adv. Mater.* **2013**, *25*, 267-272.

[30] Chen, W.; Rakhi, R. B.; Alshareef, H. N.; Morphology-Dependent Enhancement of the Pseudocapacitance of Template-Guided Tunable Polyaniline Nanostructures. *J. Phys. Chem. C* **2013**, 117, 15009-15019

[31] Roldan, S.; Blanco, C.; Granda, M.; Menendez, R.; Santamaría, R. Towards a Further Generation of High-Energy Carbon-Based Capacitors by using Redox-Active Electrolytes. *Angew. Chem., Int. Ed.* **2011**, 50, 1699-1701.

[32] Dubal, D. P.; Suarez-Guevara, J.; Tonti, D.; Enciso, E.; Gomez-Romero, P.; A high voltage solid state symmetric supercapacitor based on graphene–polyoxometalate hybrid electrodes with a hydroquinone doped hybrid gel-

electrolyte, *J. Mater. Chem. A*, **2015**, 3, 23483–23492

[33] Xiao, X.; Peng, X.; Jin, H.; Li, T.; Zhang, C.; Gao, B.; Hu, B.; Huo, K.; Zhou, J.; Freestanding Mesoporous VN/CNT Hybrid Electrodes for Flexible All-Solid-State Supercapacitors. *Adv. Mater.* **2013**, 25, 5091-5097

[34] Yuan, L. Y.; Lu, X. H.; Xiao, X.; Zhai, T.; Dai, J. J.; Zhang, F. C.; Hu, B.; Wang, X.; Gong, L.; Chen, J.; Hu, C. G.; Tong, Y. X.; Zhou, J.; Wang, Z. L.; Flexible Solid-State Supercapacitors Based on Carbon Nanoparticles/MnO_2 Nanorods Hybrid Structure. *ACS Nano* **2012**, 6, 656-661

[35] Lu, X.; Yu, M.; Zhai, T.; Wang, G.; Xie, S.; Liu, T.; Liang, C.; Tong, Y.; Li, Y.; High Energy Density Asymmetric Quasi-Solid-State Supercapacitor Based on Porous Vanadium Nitride Nanowire Anode. *Nano Lett.* **2013**, 13, 2628-2633

Figure Captions

Figure 1 Schematic illustration of steps involved in the synthesis of reduced graphene oxide (rGO) and phosphotungstate (PW_{12}) hybrid material (rGO-PW_{12}) with corresponding EDS mapping. Note that POM sketch is reproduced from our previous publication with the permission from Royal Society of Chemistry [32].

Figure 2 (a) XRD patterns of rGO and rGO-PW_{12} hybrid materials, (b) core-level XPS spectra of C1s and (c) W4f of rGO-PW_{12} sample, respectively, (d, e) SEM images and (f, g) STEM images of rGO and rGO-PW_{12} hybrid samples, respectively (h) HR-TEM image of rGO-PW_{12} sample (i) EDS spectrum of rGO-PW_{12} sample measured from TEM.

Figure 3 (a, b) CV and GCD curves for rGO and rGO-PW_{12} symmetric cells at a fixed scan rate of 20 mV/s and a constant current density of 1.27 mA/cm^2, respectively, (c, d) CV and GCD curves for rGO-PW_{12} based cells at various scan rates and current densities, respectively. (e) Plots of variation of volumetric capacitance of rGO and rGO-PW_{12} based cells with scan rates, (f) Plots of energy and power densities for rGO and rGO-PW_{12} symmetric cells.

Figure 4 (a) CV curves at various scan rates for rGO-PW_{12} symmetric cells with 0.2 M HQ doped gel-electrolyte, (b-d) CD curves of rGO-PW_{12} symmetric cells at different current densities with HQ doped gel-electrolyte of different concentrations, respectively, (e) Variation of volumetric capacitances of rGO-PW_{12} cell for different HQ concentrations with current densities, (f) volumetric energy density vs power density plots of rGO-PW_{12} symmetric cell with different concentration of HQ doped electrolytes in Ragone plot.

Figure 5 Thirty-one (31) LED indicators with word "NEO" powered rGO-PW_{12} symmetric cell with 0.2 M HQ doped polymer gel electrolyte.

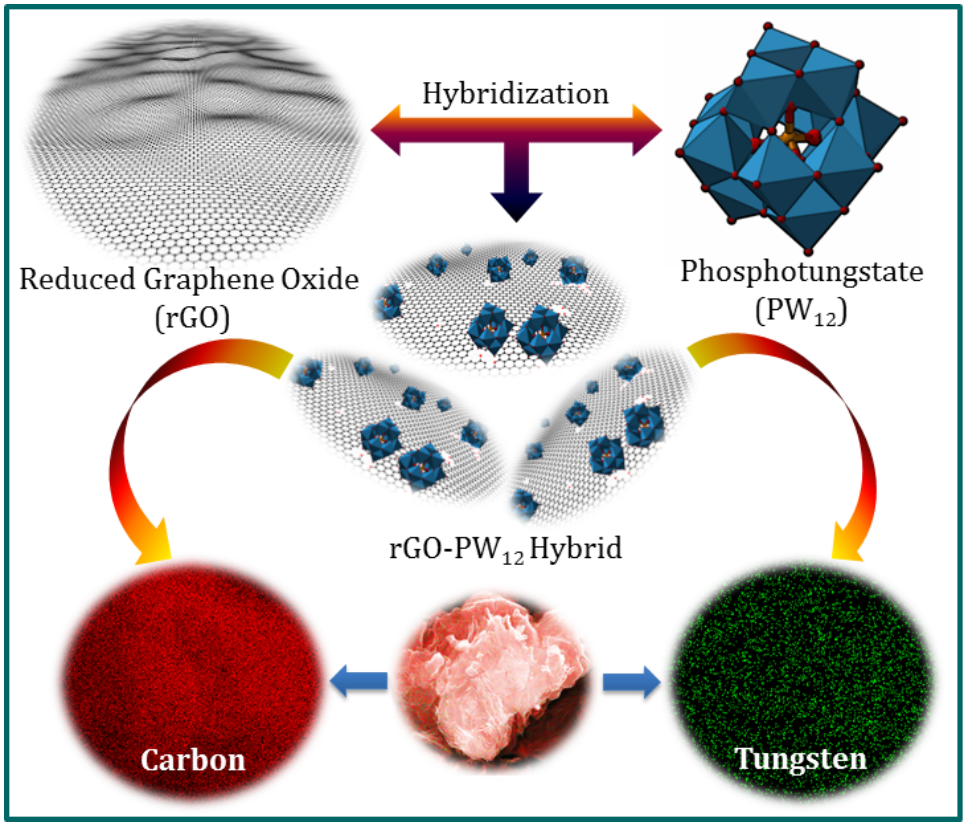

Figure 1 Schematic illustration of steps involved in the synthesis of reduced graphene oxide (rGO) and phosphotungstate (PW_{12}) hybrid material (rGO-PW_{12}) with corresponding EDS mapping. Note that POM sketch is reproduced from our previous publication with the permission from Royal Society of Chemistry [32].

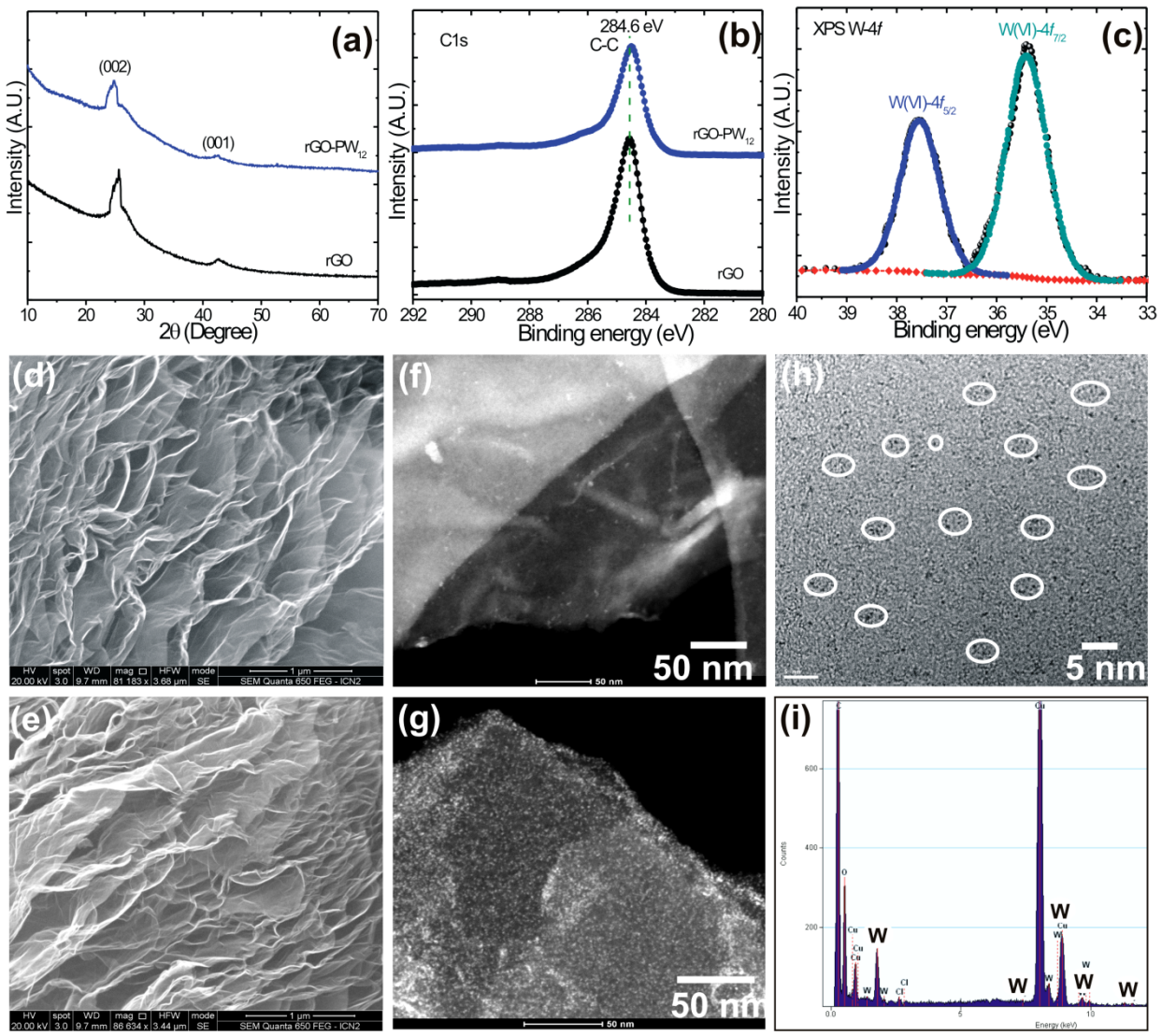

Figure 2 (a) XRD patterns of rGO and rGO-PW_{12} hybrid materials, (b) core-level XPS spectra of C1s and (c) W4f of rGO-PW_{12} sample, respectively, (d, e) SEM images and (f, g) STEM images of rGO and rGO-PW_{12} hybrid samples, respectively (h) HR-TEM image of rGO-PW_{12} sample (i) EDS spectrum of rGO-PW_{12} sample measured from TEM.

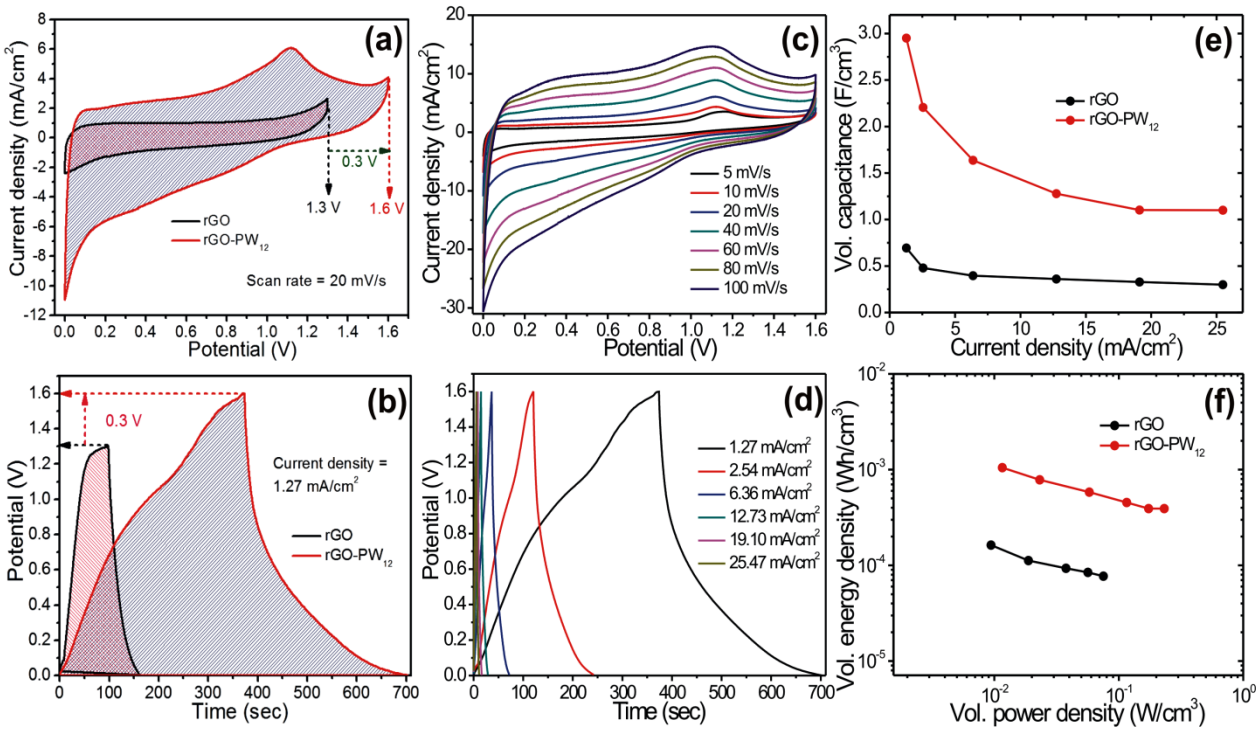

Figure 3 (a) CV curves and (b) CD curves of rGO and rGO-PW_{12} symmetric cells at scan rate of 20 mV/s and current density of 1.27 mA/cm^2, respectively, (c, d) cyclic voltammetry (CV) and galvanostatic charge/discharge (CD) curves for rGO-PW_{12} based symmetric cells at different scanning rates and current densities, respectively. (e) Variation of volumetric capacitance of rGO and rGO-PW_{12} based symmetric cells as a function of scan rates, (f) the volumetric power and energy density values of rGO and rGO-PW_{12} symmetric cells.

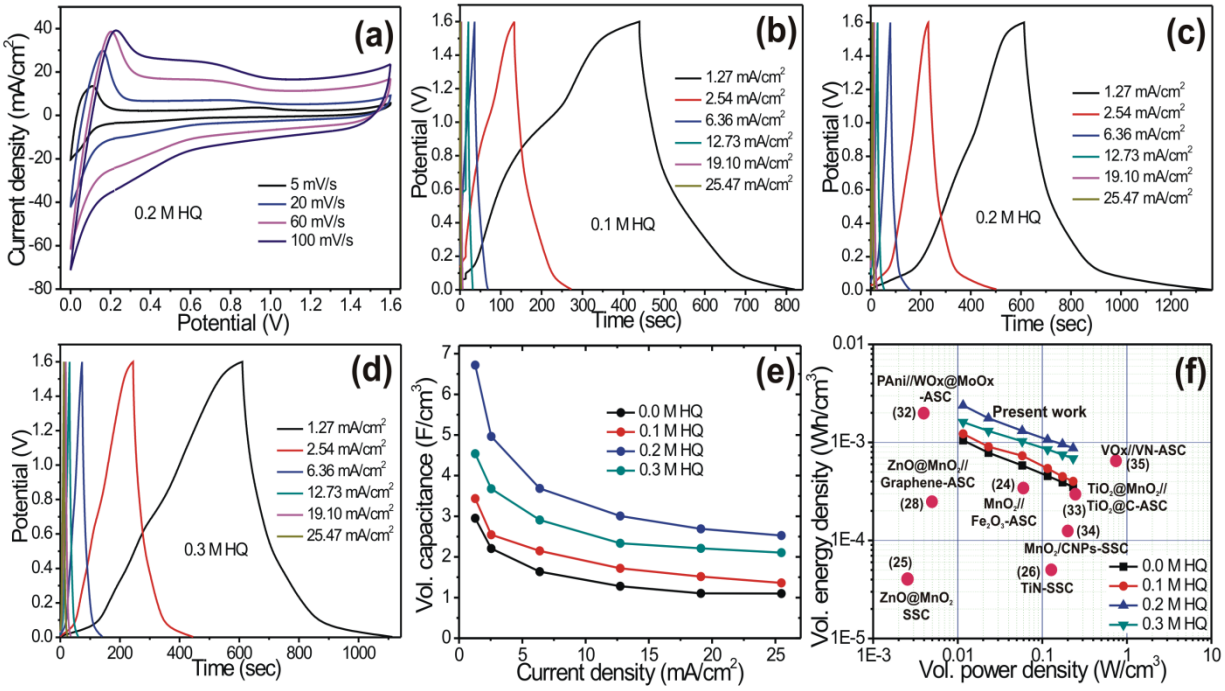

Figure 4 (a) CV curves at various scan rates for rGO-PW_{12} symmetric cells with 0.2 M HQ doped gel-electrolyte, (b-d) CD curves of rGO-PW_{12} symmetric cells at different current densities with HQ doped gel-electrolyte of different concentrations, respectively, (e) Variation of volumetric capacitances of rGO-PW_{12} cell for different HQ concentrations with current densities, (f) volumetric energy density vs power density plots of rGO-PW_{12} symmetric cell with different concentration of HQ doped electrolytes in Ragone plot,

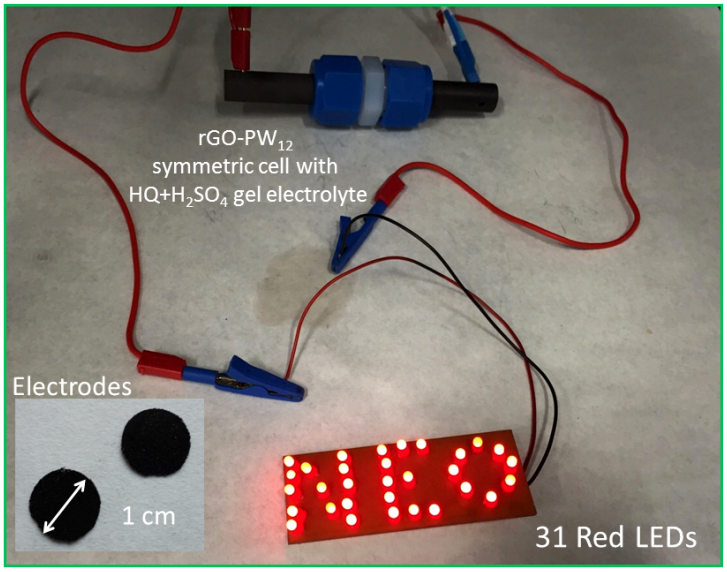

Figure 5 Thirty-one (31) LED indicators with word “NEO” powered rGO-PW_{12} symmetric cell with 0.2 M HQ doped polymer gel electrolyte.

Supporting information

Ultrahigh energy density supercapacitors through a double hybrid strategy

Deepak P. Dubal, Bhawna Nagar, Pedro Gomez-Romero ***

[a]Catalan Institute of Nanoscience and Nanotechnology (ICN2), CSIC and The Barcelona Institute of Science and Technology, Campus UAB, Bellaterra, 08193 Barcelona, Spain

CORRESPONDING AUTHOR FOOTNOTE

Dr. Deepak Dubal, and Prof. Pedro Gomez-Romero

Tel.: +349373609/+345929950 Fax: +345929951

E-mail: dubaldeepak2@gmail.com (D. Dubal),

pedro.gomez@cin2.es (P. Gomez-Romero)

Supporting information S1

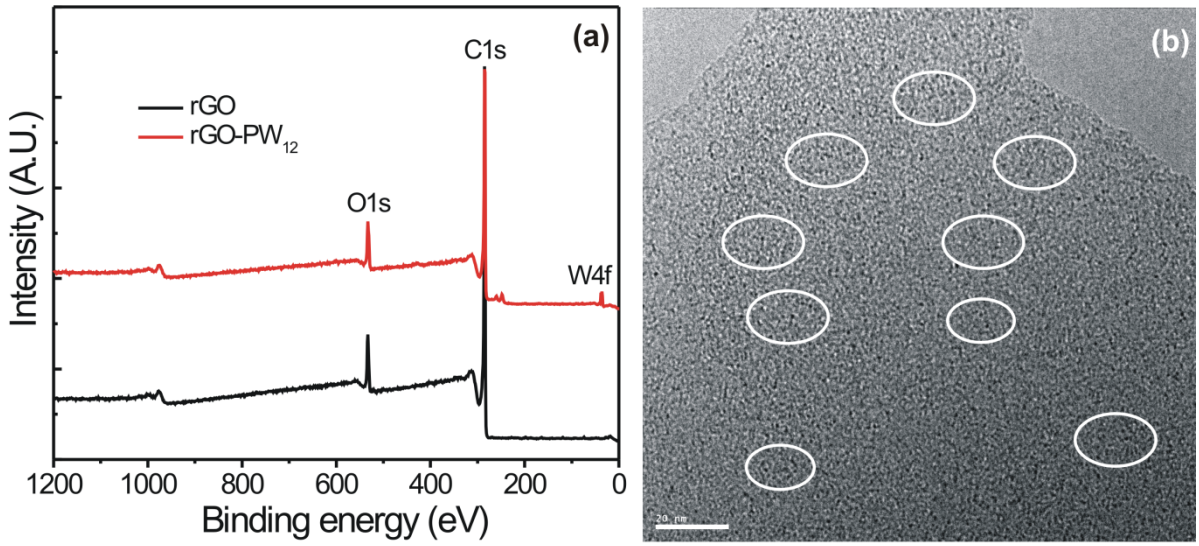

Fig. S1 (a) Full XPS spectra of rGO and rGO-PW_{12} samples, (b) HR-TEM image of rGO-PW_{12} sample.

Supporting information S2

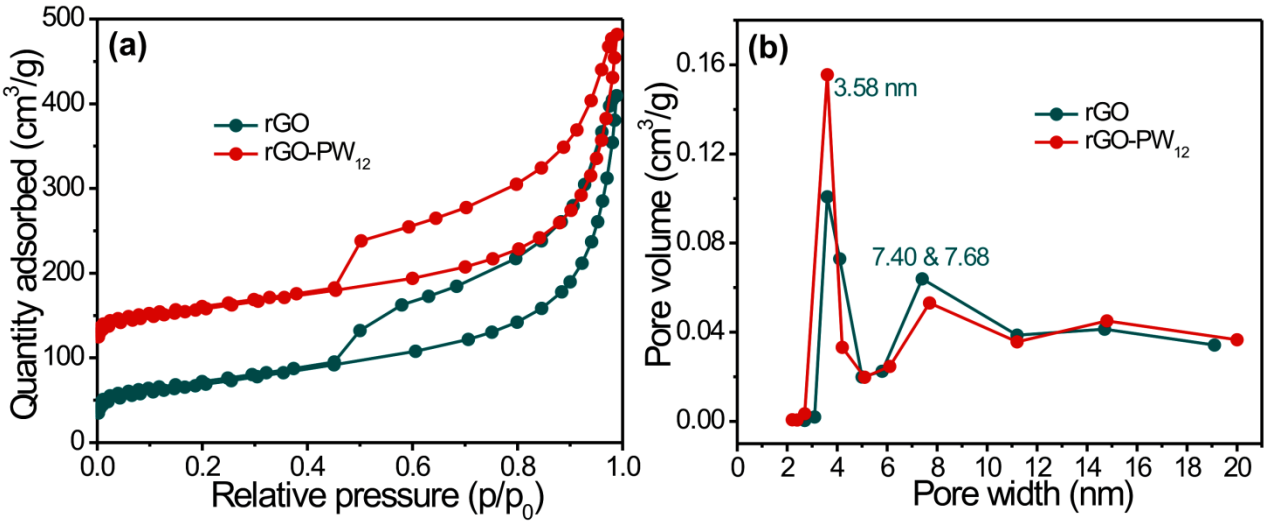

Figure S2 (a) Nitrogen adsorption-desorption isotherm of rGO and rGO-PW_{12} samples with (b) corresponding pore size distribution curves

Supporting information S3

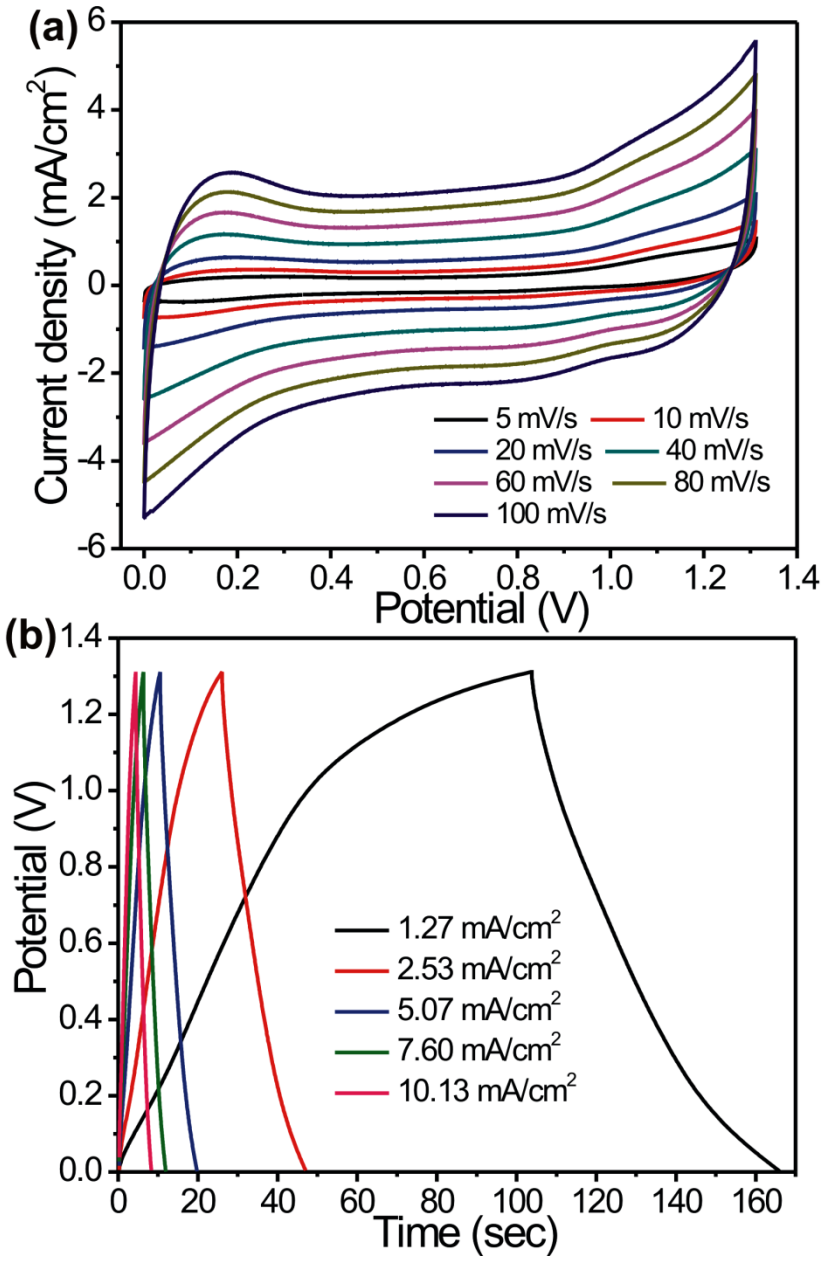

Figure S3 (a) Cyclic voltammetry curves at different scan rates, (b) Charge-discharge curves at different current densities for rGO based symmetric cell

Supporting information S4

Calculations:

The cell (device) capacitance (*C*) and volumetric capacitance of the symmetric devices were calculated from their CVs according to the following equation:

$$C_{cell} = \frac{Q}{\Delta V} \quad (1)$$

$$C_A = \frac{Q}{A \times \Delta V} \quad \text{and} \quad C_V = \frac{Q}{V \times \Delta V} \quad (2)$$

where, C_A and C_V are areal and volumetric capacitances, respectively. *Q* (C) is the average charge during the charging and discharging process, V is the volume (cm^3) of the whole device (The area and thickness of our symmetric cells is about 0.785 cm^2 (Area, $A=\pi r^2$, $3.14 \times (0.5)^2$) and 0.088 cm. Hence, the whole volume of device is about 0.069 cm^3, ΔV (V) is the voltage window. It is worth mentioning that the volumetric capacitances were calculated taking into account the volume of the device stack. This includes the active material, the flexible substrate and the separator with electrolyte.

Alternatively, the cell capacitance (C_{cell}), areal (C_A) and volumetric (C_V) capacitance of the electrode (C_V) was estimated from the slope of the discharge curve using the following equations:

$$C_{cell} = \frac{I \times \Delta t}{\Delta V} \quad (4)$$

$$C_A = \frac{I \times \Delta t}{A \times \Delta V} \quad \text{and} \quad C_V = \frac{I \times \Delta t}{V \times \Delta V} \quad (5)$$

where *I* is the applied current, V is the volume (cm^3) of the whole device (the whole volume of our device is about 0.069 cm^3), Δt is the discharging time, ΔV (V) is the voltage window.

Volumetric energy (E, Wh/cm^3) and power density (P, W/cm) of the devices were obtained from the following equations:

$$E = \frac{1}{2 \times 3600} C_V \Delta V^2 \quad (6)$$

$$P = \frac{3600 \times E}{\Delta t} \quad (7)$$

where *E* (Wh/cm^3*)* is the energy density, *CV* is the volumetric capacitance obtained from Equation (5) and *ΔV* (V) is the voltage window, P (W/cm^3) is the power density.

Supporting information S5

Table 1 Comparison on supercapacitive values of POM as well as metal oxide based electrodes

Electrode	Device	Electrolyte	Capacitance	Ref.
SWCNT-TBA-PV_2Mo_{10}	Symmetric	H_2SO_4	317 mF/cm^2	[1]
$H_3PMo_{12}O_{40}$/MWCNT	Symmetric	H_2SO_4	38 F/g	[2]
$H_3PMo_{12}O_{40}$/PPy//$H_3PW_{12}O_{40}$/PEDOT	Asymmetric	H_2SO_4	31 F/g	[3]
$H_3PMo_{12}O_{40}$/PAni	Symmetric	H_2SO_4	195 mF/cm^2	[4]
PAni/SiW_{12}	Symmetric	H_2SO_4	1.8 mF/cm^2	[5]
PAni/PW_{12}	Symmetric	H_2SO_4	15 mF/cm^2	[5]
MnO_2//Fe_2O_3	Asymmetric	Gel-electrolyte	1.21 F/cm^3	[6]
ZnO@MnO_2	Symmetric	Gel-electrolyte	0.325 F/cm^3	[7]
TiN	Symmetric	Gel-electrolyte	0.33 F/cm^3	[8]
Graphene	Symmetric	Gel-electrolyte	0.42 F/cm^3	[9]
ZnO@MnO_2//graphene	Asymmetric	Gel-electrolyte	0.52 F/cm^3	[10]
H-TiO_2@MnO_2//TiO_2@C	Asymmetric	Gel-electrolyte	0.70 F/cm^3	[11]
rGO-PW_{12}	*Symmetric*	*Gel-electrolyte*	*2.95 F/cm^3 (260 mF/cm^2)*	*Present work*
rGO-PW_{12} with HQ doping	*Symmetric*	*HQ doped*	*6.72 F/cm^3 (592*	*Present*

gel- *mF/cm^2)* *work*

electrolyte

References:

[1] Gomez-Romero, P.; Chojak, M.; Cuentas-Gallegos, A.; Asensio, J. A.; Kulesza, P. J.; Casan-Pastor, N.; Lira-Cantu, M.; Hybrid organic–inorganic nanocomposite materials for application in solid state electrochemical supercapacitors. *Electrochem. Commun.*, 2003, 5, 149-153

[2] Cuentas-Gallegos, A.; Lira-Cantu, M.; Casan-Pastor, N.; Gomez-Romero, P.; Nanocomposite Hybrid Molecular Materials for Application in Solid-State Electrochemical Supercapacitors. *Adv. Funct. Mater.*, 2005, 15, 1125-1133.

[3] Lu, X.; Zeng, Y.; Yu, M.; Zhai, T.; Liang, C.; Xie, S.; Balogun, M; Tong, Y.; Oxygen-deficient hematite nanorods as high-performance and novel negative electrodes for flexible asymmetric supercapacitors. *Adv. Mater.* 2014, *26*, 3148-3155.

[4] Yang, P.; Xiao, X.; Li, Y.; Ding, Y.; Qiang, P.; Tan, X.; Mai, W.; Lin, Z.; Wu, W.; Li, T.; Jin, H.; Liu, P.; Zhou, J.; Wong, C. P.; Wang, Z. L.; Hydrogenated ZnO core-shell nanocables for flexible supercapacitors and self-powered systems. *ACS Nano* 2013, 7, 2617-2626

[5] Lu, X. H.; Wang, G. M.; Zhai, T.; Yu, M. H.; Xie, S. L.; Ling, Y. C.; Liang, C. L.; Tong, Y. X.; Li, Y.; Stabilized TiN nanowire arrays for high-performance and flexible supercapacitors. *Nano Lett.* 2012, 12, 5376-5381.

[6] El-Kady, M. F.; Strong, V.; Dubin, S.; Kaner, R. B.; Laser scribing of high-performance and flexible graphene-based electrochemical capacitors. *Science* 2012, 335, 1326-1330.

[7] Zilong, W.; Zhu, Z.; Qiu, J.; Yang, S.; High performance flexible solid-state

asymmetric supercapacitors from MnO_2/ZnO core–shell nanorods//specially reduced graphene oxide. *J. Mater. Chem. C,* 2014, 2, 1331-1336.

[8] Lu, X.; Yu, M.; Wang, G.; Zhai, T.; Xie, S.; Ling, Y.; Tong, Y.; Li, Y.; H-TiO_2@MnO_2//H-TiO_2@C core-shell nanowires for high performance and flexible asymmetric supercapacitors. *Adv. Mater.* 2013, *25*, 267-272.

[9] Chen, W.; Rakhi, R. B.; Alshareef, H. N.; Morphology-dependent enhancement of the pseudocapacitance of template-guided tunable polyaniline nanostructures. *J. Phys. Chem. C* 2013, 117, 15009-15019

[10] Roldan, S.; Blanco, C.; Granda, M.; Menendez, R.; Santamaría, R. Towards a further generation of high-energy carbon-based capacitors by using redox-active electrolytes. *Angew. Chem., Int. Ed.* 2011, 50, 1699-1701.

[11] Xiao, X.; Peng, X.; Jin, H.; Li, T.; Zhang, C.; Gao, B.; Hu, B.; Huo, K.; Zhou, J.; Freestanding mesoporous VN/CNT hybrid electrodes for flexible all-solid-state supercapacitors. *Adv. Mater.* 2013, 25, 5091-5097

Supporting information S6

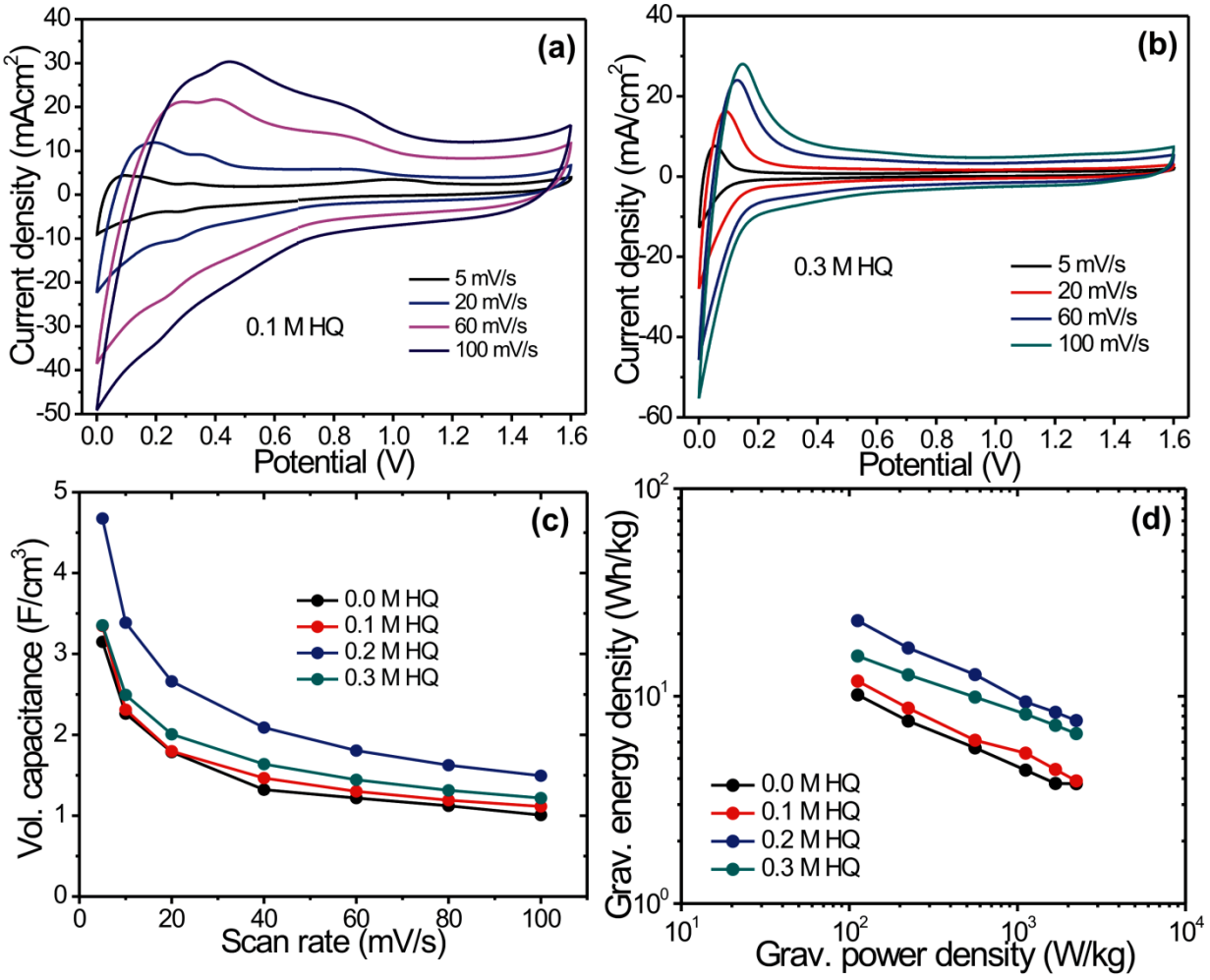

Figures S6 (a, b) CV curves of rGO-PW_{12} symmetric cell at different scan rates with HQ doped polymer gel-electrolyte with different concentrations. (c) Variation of volumetric capacitances of rGO-PW_{12} symmetric cell with scan rate for HQ doped polymer gel-electrolyte of different concentration, (d) Summary of volumetric energy and power of rGO-PW_{12} cell in Ragone plot for HQ doped polymer gel-electrolyte of different concentration

Supporting information S7

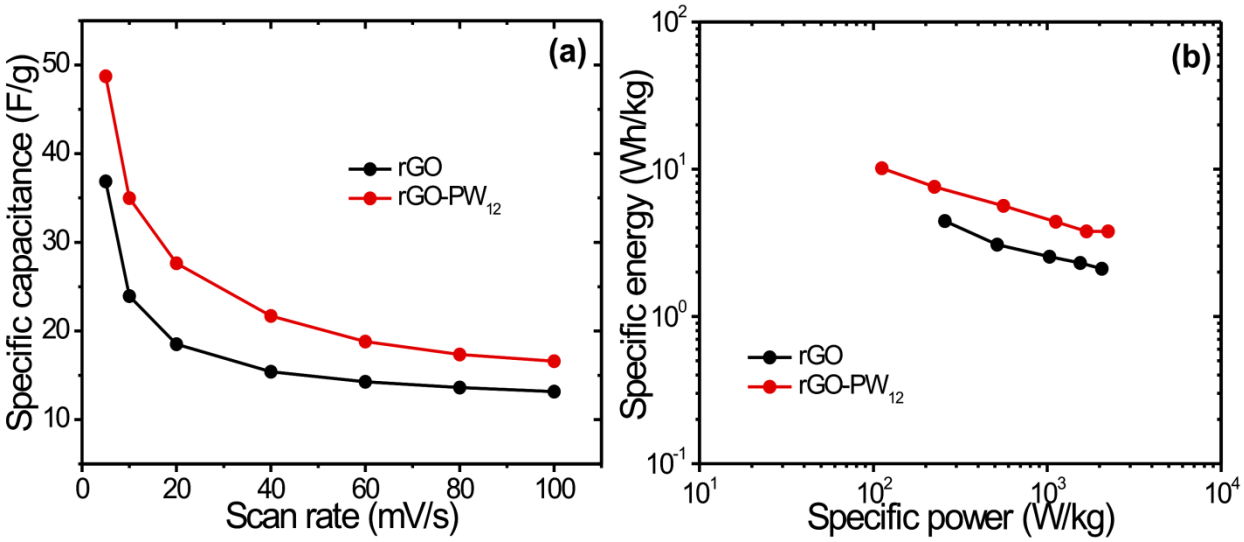

Figure S7 (a) Variation of specific capacitance with scan rates for rGO and rGO-PW_{12} symmetric cells, (b) Summary of specific energy and specific power for rGO and rGO-PW_{12} symmetric cells

Supporting information S8

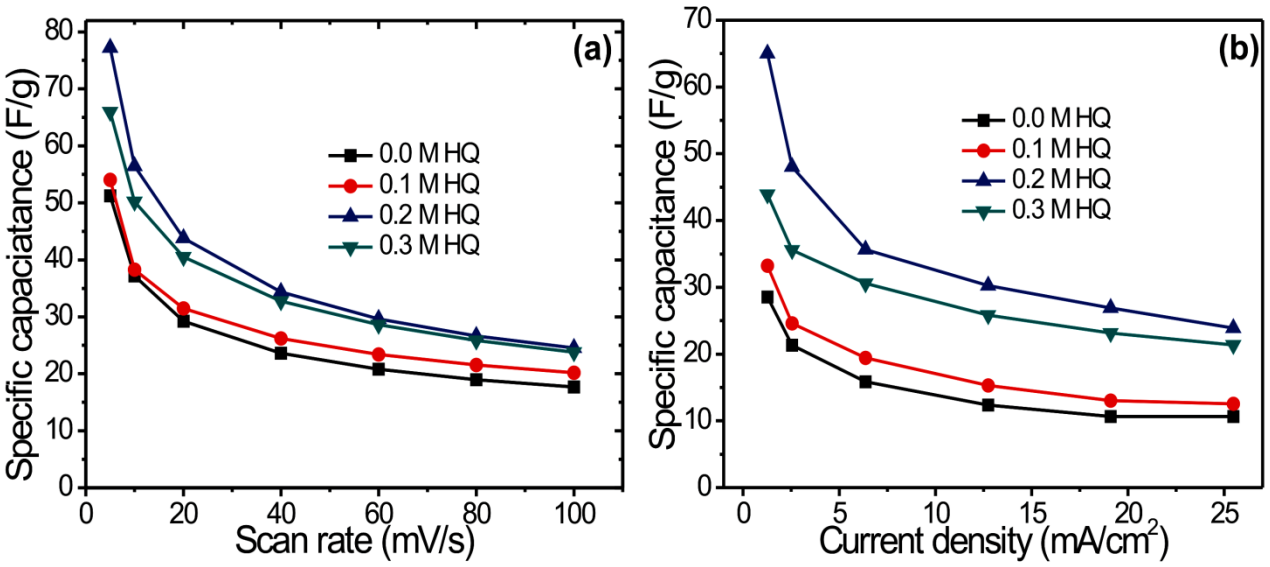

Figure S8 (a, b) Variation of specific capacitance of rGO-PW_{12} symmetric cells with scan rates and current densities for HQ doped gel electrolyte of different concentrations, respectively.

Research Highlights

- Double Hybrid Approach with Hybrid electrode and hybrid electrolyte
- Introducing redox-active gel-electrolyte
- Excellent volumetric capacitances
- Ultrahigh energy density